Systems & Control Transactions

Original Research Article
Peer Reviewed Conference Proceeding
ESCAPE 36 - European Symposium on Computer Aided Process Engineering
Sheffield, UK. 21-24 June 2026

PSE PRESS

Structural Constraints with the P-graph Framework: Application to an Ammonia Synthesis Process

Darrick Hillaby[a], Andrés Piña Martinez[a]*, Jean-François Portha[a]*, and Laurent Falk[a]

[a] Université de Lorraine, CNRS, LRGP, Nancy, F-54000, France
* Corresponding Authors: andres-david.pina-martinez@univ-lorraine.fr, jean-francois.portha@univ-lorraine.fr.

ABSTRACT

An optimized flowsheet can be generated by numerous approaches. Process optimization via superstructure is one of the methods used to provide solutions that consider the interactions between different decision layers. A process simulator-based optimization is considered in this work, as it offers a reliable and rigorous modeling environment. It is then coupled with a P-graph-based framework to reduce the tedious mathematical writing of the logical constraints to guarantee the structural coherence of a sequence of unit operations.The developed framework consists of three algorithms. The first algorithm transforms the superstructure flowsheet into a P-graph. The second algorithm gets process sub-structures from the superstructure by searching for active units corresponding to a set of decisions made, for example, by an optimizer. The third one checks structural feasibility by verifying that the resulting structure satisfies the five axioms of the original P-graph framework and two additional connectivity tests proposed in this work.The proposed methodology is then applied to an ammonia synthesis process. The results obtained in this work enable a reduction in structural logical constraints while achieving outcomes equivalent to those of a previous study, proving the methodology's efficacy.

Keywords: Process simulator-based optimization, superstructure, P-graph framework, process synthesis, MINLP problem

INTRODUCTION

Climate ambition announced at COP28 requires drastic actions to be taken, such as tripling global renewable energy capacity and doubling the global average annual rate of energy efficiency improvements [1]. One solution to achieve the ambition is the use of modular and flexible plants [2]. Robust processes capable of handling variable inputs, flexible capacity, product variations and decentralized plants are highly valuable to the modern industry. However, modular processes require robust design methods and different optimization strategies as they must adapt to variable inputs or process parameters while maintaining increasing process efficiency. It is therefore essential to employ process design techniques, specifically process synthesis, to design modular processes.

Process synthesis is the selection and interconnection of units involving physical and chemical phenomena to obtain products from raw materials to satisfy economic, environmental and/or social objectives [3]. Main approaches include hierarchical decomposition, mathematical programming and even hybrid approaches combining both heuristics and mathematical programming. Mathematical programming-based strategies rigorously search through a proposed design space for the optimal configuration, unlike hierarchical decomposition. Depending on the definition of the search space, mathematical approaches can be categorized as superstructure-based or superstructure-free optimization [4, 5]. The superstructure-based approach consists of (a) postulating a set of process alternatives in superstructure form, (b) formulating it as a mathematical programming model, and (c) determining the optimal configuration with an optimization algorithm. Conversely, superstructure-free approaches create new flowsheets either from existing ones or from scratch.

In superstructure-based process synthesis, the superstructure can be modeled with different levels of detail. Models can be characterized into three main categories: high-level aggregate, shortcut, and detailed rigorous models. When detailed modelling is required, process

simulators offer a reliable and rigorous modeling environment [6]. In this context, superstructure optimization may be performed in two ways: in an external optimization environment or as a flowsheet in the process simulator itself.

This work focuses on the latter. To avoid extensive mathematical formulations for ensuring structural coherence, a P-graph-based framework is proposed [7]. The process superstructure is implemented in a simulator with the defined optimization problem (objective function, variables, and constraints). As shown in **Figure 1**, a P-graph-based feasibility block interacts with the simulator and an external optimizer to obtain the optimal solution. This feasibility block can be further decomposed into three algorithms.

The paper is structured as follows. First, the methodology is presented, including definitions and algorithm descriptions. Next, its application to an ammonia synthesis process is outlined. Finally, the approach is evaluated against a non–P-graph method, and the optimization results are discussed.

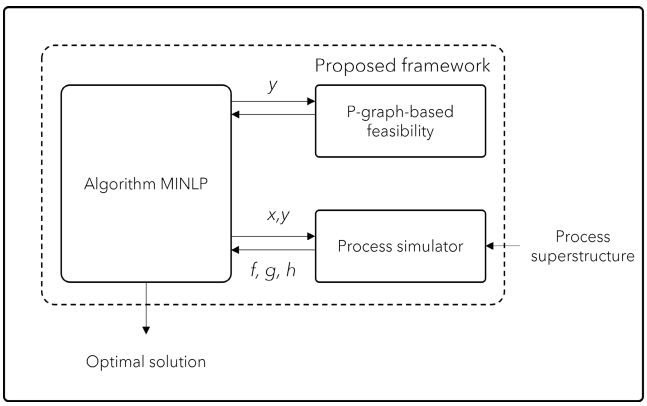

Figure 1. P-graph integrated into a process simulator-based optimization approach. Figure taken from Hillaby et al. [8].

METHODOLOGY

The P-graph-based framework proposed intends to improve the generic optimization procedure by: (1) implicitly postulating the structural constraints through the superstructure topology, (2) incorporating three procedures or algorithms, to evaluate the structural feasibility of a given process throughout the optimization. The improved methodology enables general users to leverage P-graph without requiring a direct knowledge of it. There are different technical terms that are defined in this work: permanent and conditional units; opening and closing switches; conditional stream; bypass units; structural feasibility.

Permanent and conditional units

Permanent units are defined as essential components of the structure, meaning they are necessary for the operation of the process and cannot be removed without compromising its functionality. Conditional units, on the other hand, are units that can be added or modified to optimize the structure. These units are introduced to explore different configurations or improvements in the process. If conditional units are removed, the result is the simplest or base case of the process.

Conditional, opening switch, and closing switch

The only intricacy that exists between a typical process simulator flowsheet and a P-graph process representation is the addition of a fictive operating unit or a bypass unit, herein labeled UF. Since a P-graph is a bipartite graph, a material cannot be connected to a material, hence for a structural switch that has a bypass (i.e., the material input and the material output are equal), a bypass unit has to be defined. Technically, no material transformation is done, it is only to respect the P-graph bipartite representation and its eventual algorithm that will be used. When an opening switch is identified, the directly connected streams are treated as candidate or conditional streams. This implies that, among the alternative pathways, only one stream can be activated at a time. An opening switch is a fictive unit that indicates that a decision has to be made among two candidate pathways. A close switch is also a fictive unit that requires a decision to be made from two candidate streams, coming from the same or different opening switches.

Bypass units

Bypass units are fictive units used to represent material flows that bypass any transformation processes. In other words, these units are used to model situations where a material goes directly from one point to another without undergoing any changes. However, as explained before, in a P-graph representation, the connection of one material node to another is not possible. Therefore, a bypass unit is introduced to facilitate this representation.

Structural feasibility

A feasible structure indicates that the process network adheres to the principles and logic of process synthesis, meaning that the arrangement of process units and material flows forms a valid and functional sequence. In the context of P-graph framework, a feasible structure implies that the five axioms are satisfied. For example, materials must flow into operating units, and these units must either produce outputs that feed into other units or generate final products. The maximal structure generated by the Maximal Structure Generation (MSG) method ensures that the search space is defined, from which the

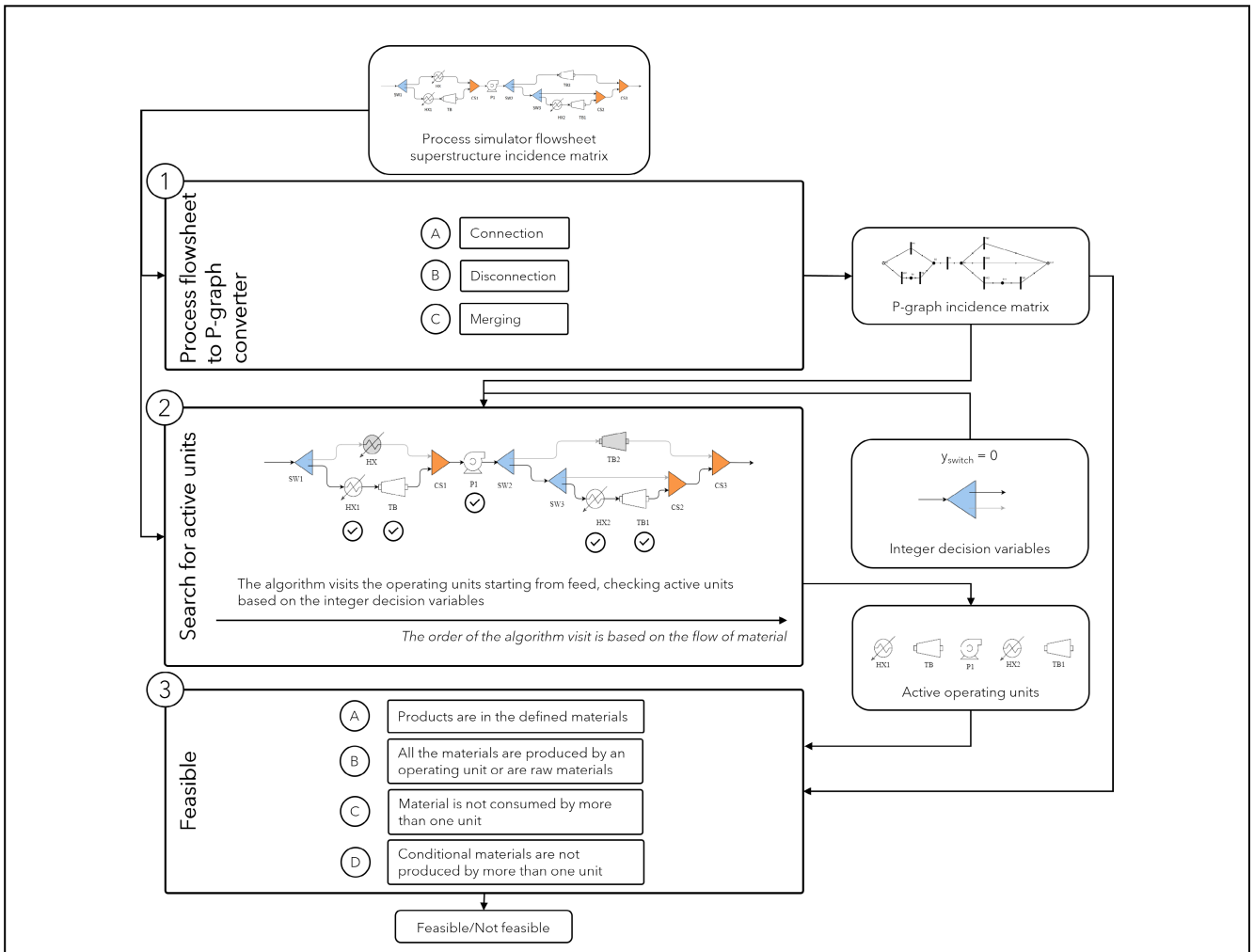

Figure 2. P-graph-based framework proposed, with three algorithms in three different blocks, labeled 1, 2, and 3. Figure adapted from Hillaby et al. [8].

optimal solutions can be identified.

MSG consists of two phases: the reduction phase and the composition phase. The algorithm used in the reduction phase is central to the methodology, with additional modifications to enhance compatibility with structural switches (i.e., opening and closing switches). The algorithm begins by extracting the information of the raw materials, products, and the superstructure (the potential arrangement of material flows and operating units). The algorithm initiates by performing the first feasibility test: verifying whether the defined products exist within the superstructure. The second test ensures that there are no intermediate products that are neither produced by any operating unit nor specified as raw materials, thus preventing the creation of unaccounted-for materials. These two tests enforce the five axioms of the P-graph framework. The third and fourth tests are added modifications, which ensure that when an opening structural switch is encountered, a decision must be made to select only one process path. Similarly, when a closing structural switch is encountered, a choice is required, meaning only one path can be accepted to continue the process sequence.

Algorithms

In general, a process optimization via superstructure starts with the user generating the superstructure itself. The problem is then defined in the simulator's optimizer interface, i.e., objective functions, constraints, and action variables. Depending on the commercial simulator used, an external optimizer could be coupled with it because the optimization tools provided by default may not be as effective or as flexible as necessary. The action variables are then assigned by the optimizer, presenting a new configuration of the flowsheet. This new structure then gets checked for feasibility. If the structure is infeasible, a penalty is applied. On the other hand, if it is feasible, the objective function is evaluated. The algorithm reassigns new action variables or exits the loop, depending on the stopping criteria such as the maximum number of evaluations, optimization time limit, or tolerance on the objective function. As the loop exits, the optimal values

are assigned and the final optimization report is obtained.

Block 1 corresponds to the Process Flowsheet to P-graph algorithm. This procedure converts a process adjacency matrix into an incidence P-graph matrix. There are three main operations that are executed: (1) connection between two units, i.e., disconnection between a unit and an open switch or a close switch (3) merging close switches' inputs.

Once the P-graph superstructure is obtained, it is possible to determine the process structure defined by the binary variables assigned by the optimizer (block 2). This is achieved by employing a graph traversal algorithm such as Depth-First Search (DFS) algorithm. The active operating units are determined and sent to the final algorithm.

Finally, the current process structure is then checked for structural feasibility (block 3). Four tests are done to ensure the structure the new process structure is feasible:

1. The products of the new structure are found in the initial defined materials.
2. All the streams are produced by an operating unit or they are defined as raw materials.
3. A stream is not consumed by more than one unit.
4. Conditional streams are not produced by more than one unit.

If the four conditions are respected, the process structure is considered structurally feasible.

By integrating the framework, i.e., the three main blocks shown in **Figure 2**, into the complete process optimization via superstructure procedure, the need to manually define structural constraints is reduced, decreasing human intervention at the start of the process simulator-based optimization. This procedure is iterative and continues until the optimization criteria are met.

A list of feasible sub-structures can be made by implementing the 2nd and 3rd algorithm blocks prior to the optimization. This precomputation reduces redundancy during the optimization stage, as repeatedly proposed structures need not be revalidated. For example, if a known feasible sub-structure is suggested multiple times by the optimizer, feasibility can be confirmed by referring to the precomputed list, instead of running the full evaluation.

AMMONIA SYNTHESIS SUPERSTRUCTURE

A case study based on Quintero-Masselski's work [9] on optimizing the Haber-Bosch (HB) process through reactors configurations is conducted to apply the developed methodology. The original ammonia process superstructure is restructured and the MINLP formulation is modified to adapt to the methodology developed. The adapted structure is shown in **Figure 3**.

Hydrogen and nitrogen from renewable sources are used to produce ammonia, which is then separated and stored. The feeds enter at 10 bar and 293.15 K and are compressed to match reaction conditions, with pressures ranging from 50 to 200 bar.

The reaction stage has different structural alternatives of adiabatic reactors, including Adiabatic Indirect Cooling Reactor (AICR) and Adiabatic Quench Cooling Reactor (AQCR). In the AICR configuration, a heat exchanger is used between the reactors to cool down the outlet stream of each reactor to the desired temperature of the following unit. This is achieved by using an external utility. In the AQCR configuration, the heat exchange is carried out by mixing the outlet stream of each reactor with a fraction of fresh process stream that is not used for reaction and bypassed from the previous reactors. There are five configurations that are implemented in the current work: (1) 1 reactor without cooling, (2) 2 adiabatic reactors in AICR configuration, (3) 3 reactors in AICR configuration, (4) 2 reactors in AQCR configuration, and (5) 3 reactors in AQCR configuration.

Iron-based (Fe) and ruthenium-based (Ru) catalysts are considered due to their industrial relevance and extensive literature availability. Process configurations (binary switches) and catalyst selection (integer variable) are modeled as discrete decision variables, as summarized in **Table 1**.

Separation by condensation is achieved by adjusting the reactor outlet mixture to its dew-point temperature, thereby separating a liquid phase composed of 99.95 % vol. ammonia with trace amounts of hydrogen and nitrogen.

These configurations are evaluated using two key performance indicators: Global Levelized Cost of Ammonia production (LCOA) and energetic efficiency. Two optimizations were performed: without the P-graph and with the P-graph methodology. The LCOA is the price of ammonia production considering every cost involved in the process, i.e., the sum of investment and operational expenditures of raw materials, electricity, and equipment.

$$\eta_E = \frac{(\dot{m}_{NH_3} LHV_{NH_3}) + \Delta\dot{W}^- + \Delta\dot{Q}^-}{(\dot{m}_{H_2} LHV_{H_2}) + \Delta\dot{W}^+ + \Delta\dot{Q}^+} \quad (1)$$

The Pré-Estime method is used to calculate the equipment cost [10]. The process energy efficiency indicator, Eq. (1), is the ratio between the useful produced energy and the supplied energy to the process: where η_E is the overall energy efficiency, $\dot{m}$ is the mass flowrate in kg/s, LHV is the Low Heating Value in kJ/kg, $\Delta\dot{W}$ is the overall balance of mechanical power in kW, and $\Delta\dot{Q}$ is the balance of thermal energy in kW. The energy terms use superscripts to indicate production (+) and consumption (-) [11].

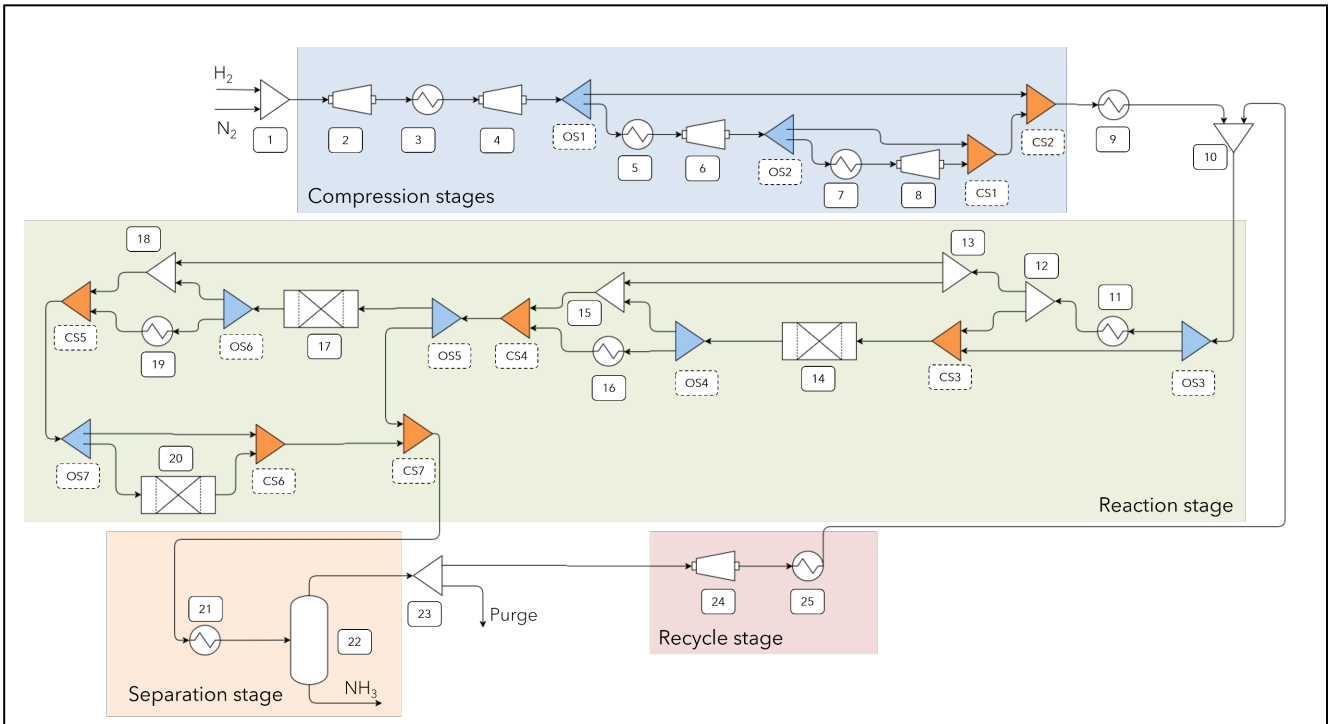

Figure 3. Superstructure representation for the evaluation of the adiabatic reactor configuration. The compression stage includes the selection of the number of compressors. The reaction stage has five structural variables to determine the number of reactors and the type of colling. Module nomenclature corresponds to: Mixers (1, 10, 15, 18), Splitters (12, 13, 23), Compressors (2, 4, 6, 8, 24), Heat exchangers (3, 5, 7, 9, 11, 16, 19, 21, 25), Adiabatic reactors (14, 17, 20), Separation drum (22), Opening switches (OS1, OS2, OS3, OS4, OS5, OS6, OS7), and Closing switches (CS1, CS2, CS3, CS4, CS5, CS6, CS7).

There are seven inequality process constraints that are defined in this problem, see **Table 2**. The maximum LCOA is fixed to discard solutions with high costs of production whereas the minimum H2 conversion is defined to avoid low H1 conversions per pass and important hydrogen losses on the purge stream. A maximal reactor temperature is defined to increase the catalyst lifetime.

Table 1. Discrete action variables defined in this study.

Variable	Details
SW1	Enables the 3rd compressor
SW2	Enables the 4th compressor
SW3	Enables the quench setting
SW4	Enables either the 1st quench or the 1st external cooling heat exchanger
SW5	Enables the 2nd reactor
SW6	Enables the 2nd quench or the 2nd external cooling heat exchanger
SW7	Enables the 3rd reactor
Catalyst	0: Fe-based; 1: Ru-based

Table 2. Process constraints and their values, with the catalysts' corresponding pressure intervals being the disjunctive constraints.

Constraint	Value	Units
Maximum LCOA	850	€/t
Minimum H_2 global conversion	90	%
Maximal temperature in 1st reactor	800	K
Maximal temperature in 2nd reactor	800	K
Maximal temperature in 3rd reactor	800	K
Fe catalyst pressure range	150 – 250	bar
Ru catalyst pressure range	50-100	bar

The optimizer handles the constraint violations in two layers: internally and externally. The first layer is an external layer, in which the structural feasibility is assessed. If the structure is not feasible, i.e., the P-graph axioms are violated, a death penalty (objective functions, $f(x) = 10^{300}$; constraints, $g(x) = 0$) is applied.

The second layer is the internal layer, in which the Oracle Penalty Method [12] is applied. If the candidate solutions are structurally feasible, the method ranks the solutions using both objective value and constraint residual.

Table 3. Continuous action variables defined in the optimization, together with the stage at which they are defined, the associated process units, and their bounds.

Variable	Stage	Process unit	Bounds	Units
Pressure	Compression	2, 3, 6, 8	50 – 200	bar
Inlet temperature at 1st reactor	Reaction	9, 25	636 – 736	K
Inlet temperature at 2nd reactor	Reaction	16	636 – 736	K
Inlet temperature at 3rd reactor	Reaction	19	636 – 736	K
Length of 1st reactor	Reaction	14	0.5 – 7.0	m
Length of 1st reactor	Reaction	17	0.5 – 7.0	m
Length of 1st reactor	Reaction	20	0.5 – 7.0	m
Separation temperature	Separation	21	253 – 275	K
Split ratio at first quench splitter	Reaction	12	0.4 – 0.8	-
Split ratio at second quench splitter	Reaction	13	0.4 – 0.8	-

Implementation

The optimizations were performed on ProSimPlus 3.7.9 coupled with an external optimizer (MIDACO [13]) on an Intel(R) Xeon(R) w5-3433, 1.99 GHz, 256 GB RAM, Windows 10 64-bit operating system. The optimizations stopped when 15000 consecutive evaluations no longer improved the current solution. The optimization is done with two seeds, improving the exploration of the search space and reduce sensitivity to stochastic convergence.

RESULTS

Methodology comparison

Table 4. A comparison of the optimal point intervals between Quintero-Masselski's study [9] and this work.

Catalyst	Objective functions	Quintero-Masselski	This work
Fe	LCOA (€/t)	752 – 816	751 – 753
	Efficiency (%)	54.4 – 56.4	53.9 – 54.8
Ru	LCOA (€/t)	754 – 804	752 – 804
	Efficiency (%)	55.3 – 58.1	54.8 – 58.2

Based on the results of the optimizations performed, as shown in **Table 4**, it can be said that the modified superstructure is equivalent to the one used in Quintero-Masselski's work [9]. Hence, only the comparison between optimizations done with and without the modified P-graph methodology is done hereinafter.

The runs without the P-graph procedures and with the proposed methodology (P-graph based) took 47.7 and 36.6 hours respectively, resulting in a 22 % reduction of optimization time. The results are further detailed in **Table 5**.

90 % of the solutions proposed by the optimizer with the P-graph-based methodology implemented are feasible structurally, representing most of the evaluations performed. This is because a death penalty is applied when the solution proposed is deemed infeasible, steering the optimizer toward a feasible region. The percentage of simulator-feasible solutions among the structurally feasible points, represented by $\frac{n_{simF}}{n_{structF}}$, is similar for both cases. This suggests that the structural feasibility had more impact on the simulator convergence than the combination of continuous action variables for a given candidate design. Finally, the methodology shows a clear advantage when comparing the fraction of design-feasible over simulator-feasible solutions, at 0.94 over 0.68.

Furthermore, based on **Figure 4**, there are 45 global Pareto points, of which 35 are with P-graph and 10 are without P-graph. This shows that more non-dominated Pareto points are attained with the modified methodology.

Table 5. Comparison of the methodology with different fractions to analyze the efficacy of the methodology, including structural-feasible over total data points (3rd column), simulation-feasible over structural-feasible (4th column), and design-feasible over simulation-feasible (5th column).

Case	n_D	$\frac{n_{structF}}{n_D}$	$\frac{n_{simF}}{n_{structF}}$	$\frac{n_{designF}}{n_{simF}}$
Without P-graph	27397	0.27	0.96	0.68
With P-graph	18053	0.90	0.94	0.94

Process optimization discussions

There are several interpretations that can be considered as an extended version to that of Quintero-Masselski and colleagues' work. Only the results from the P-graph methodology are studied in this section.

Figure 5 shows that the two-compressor configuration dominates the lower efficiency and lower LCOA zone

whereas the three-compressor and a four-compressor configurations zone are mostly overlapped. This indicated that the main performance gain in energy efficiency comes from increasing the compressor number to at least three stages, while a fourth stage provides limited improvement. But increasing the number of compressors will increase the LCOA.

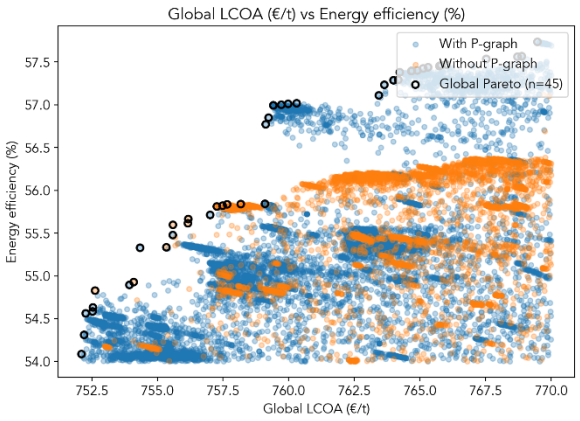

Figure 4. Energy efficiency vs. process LCOA. Blue points correspond to solutions obtained with the P-graph methodology, orange points to solutions obtained without it. Pareto-optimal points are shown as hollow black markers.

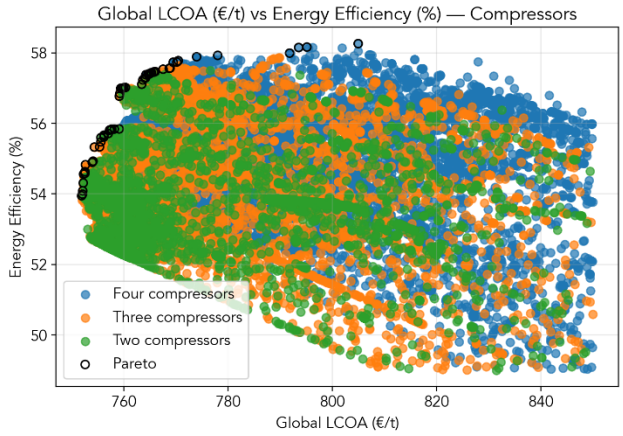

Figure 5. LCOA versus process energy efficiency, colored by the number of compressors (2, 3, or 4). Global Pareto-optimal solutions are indicated by hollow black markers.

Figure 6 exhibits that the configurations with 1, 2 or 3 AICR dominates the solution space as 2 and 3 AQCR are not as visible in the figure. When comparing the AICR configurations, the systems with 1 reactor have clearly the lower efficiency and the lower LCOA values. When there is only one stage of reaction, this means lower conversion per pass, requiring massive recycle load and increasing recycle compressor duty.

Figure 7 compares the solutions based on the type of catalyst used. There are 36643 and 44363 solution points for the Fe-based and the Ru-based catalysts respectively. There are 8 solutions on the Pareto front with Fe-catalyst ranging from 752 to 753 €/t in LCOA and from 53 % to 55 % in energy efficiency while 47 Ru-based solutions on the Pareto front ranging from 752 to 805 €/t in LCOA and from 55 % to 58 %. The increased value of energy efficiency using Ru can be explained by a lower pressure range which lead to a decrease in the compression power.

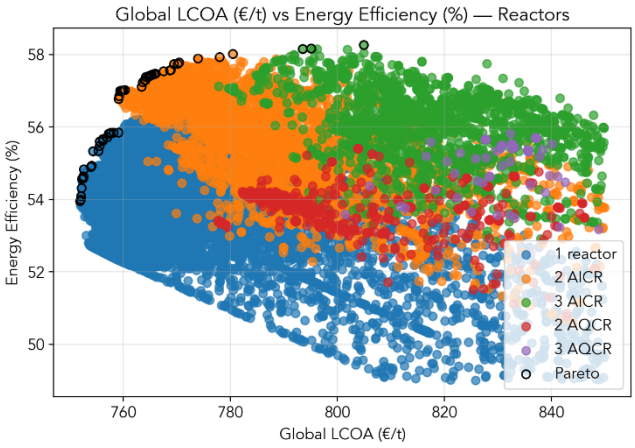

Figure 6. LCOA versus process energy efficiency, colored by the number (1, 2, or 3) and configuration (with or without cold shot) of reactors. Global Pareto-optimal solutions are indicated by hollow black markers.

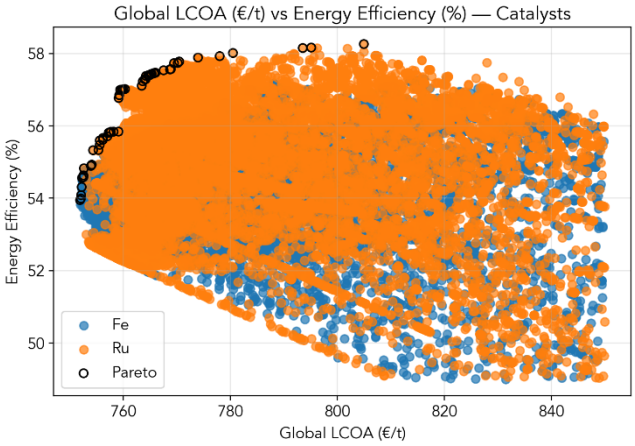

Figure 7. LCOA versus process energy efficiency, colored by the type of catalysts (Fe-based or Ru-based). Global Pareto-optimal solutions are indicated by hollow black markers.

CONCLUSION

This work demonstrates a novel methodology of process simulator-based optimization via superstructure with an application for ammonia synthesis through the Haber Bosch process.

Binary opening and closing switches as well as three algorithms are introduced in this study. The binary switches are used to propose different structural alternatives in a process while the three algorithms are used to determine the feasibility of sub-structures in a superstructure.

The approach proposed not only reduced the time required to optimize a process superstructure, especially when comparing the total evaluated solutions that are design-wise feasible but also reduced the need for users to define the structural constraints.

Future work is going to be more focused on benchmarking additional case studies using the proposed methodology, as well as conducting a more holistic optimization in which a Key Performance Indicator (KPI) of the Life Cycle Assessment (LCA) is included in the objective functions.

ACKNOWLEDGEMENTS

The authors address their acknowledgements to Jean Pimentel Losada of the Budapest University of Technology and Economics, for his valuable insights concerning the P-graph framework.

AUTHOR IDENTIFIERS

Author ORCIDs:
Hillaby D.: 0009-0007-0721-3972
Piña Martinez A.: 0000-0003-0691-0075
Portha J.-F.: 0000-0001-8698-8635

REFERENCES

1. UNFCCC, Summary of Global Climate Action at COP 28, 2023. https://unfccc.int/documents/636485
2. Montastruc L, Belletante S, Pagot A, Negny S, Raynal L. From conceptual design to process design optimization: a review on flowsheet synthesis. Oil Gas Sci. Technol. – Rev. IFP Energies nouvelles 74:80 (2019). https://doi.org/10.2516/ogst/2019048
3. Chen Q, Grossmann IE. Recent developments and challenges in optimization-based process synthesis. Annu. Rev. Chem. Biomol. Eng. 8:249-283 (2017). https://doi.org/10.1146/annurev-chembioeng-080615-033546
4. Mencarelli L, Chen Q, Pagot A, Grossmann IE. A review on superstructure optimization approaches in process system engineering. Computers & Chemical Engineering 136:106808 (2020). https://doi.org/10.1016/j.compchemeng.2020.106808
5. Boonstra S, van der Blom K, Hofmeyer H, Emmerich MTM, van Schijndel J, de Wilde P. Toolbox for super-structured and super-structure free multi-disciplinary building spatial design optimisation. Advanced Engineering Informatics 36:86-100 (2018). https://doi.org/10.1016/j.aei.2018.01.003
6. Corbetta M, Grossmann IE, Manenti F. Process simulator-based optimization of biorefinery downstream processes under the generalized disjunctive programming framework. Computers & Chemical Engineering 88:73-85 (2016). https://doi.org/10.1016/j.compchemeng.2016.02.009
7. Friedler F, Orosz Á, Pimentel Losada J. P-graphs for process systems engineering. Springer International Publishing (2022). https://doi.org/10.1007/978-3-030-92216-0
8. Hillaby D, Piña-Martinez A, Falk L, Portha JF. Structural constraint reduction in process simulator-based optimisation: leveraging the p-graph framework. Computers & Chemical Engineering 201:109254 (2025). https://doi.org/10.1016/j.compchemeng.2025.109254
9. C.S. Quintero-Masselki, Process design by superstructure optimization for the industry of the future, Université de Lorraine, 2022.
10. A. Chauvel, G. Fournier, C. Raimbault, A. Pigeyre, Manual of Process Economic Evaluation, Éditions Technip, Paris (2001).
11. Peduzzi E, Boissonnet G, Haarlemmer G, Maréchal F. Thermo-economic analysis and multi-objective optimisation of lignocellulosic biomass conversion to fischer–tropsch fuels. Sustainable Energy Fuels 2:1069-1084 (2018). https://doi.org/10.1039/c7se00468k
12. Schlüter M, Gerdts M. The oracle penalty method. J Glob Optim 47:293-325 (2009). https://doi.org/10.1007/s10898-009-9477-0
13. Schlüter M, Egea JA, Banga JR. Extended ant colony optimization for non-convex mixed integer nonlinear programming. Computers & Operations Research 36:2217-2229 (2009). https://doi.org/10.1016/j.cor.2008.08.015